

UNSTEADY FLOW APPLICATIONS IN WATERWAYS¹

February 1983

Almost all flow in waterways is to some extent unsteady, i.e., it changes with time. Also, the rate of flow and the depth usually vary along the length of the waterway. The extent of flow variation with time and distance may be such that steady flow may be assumed for very limited conditions. Sometimes and in certain applications, the flow may be assumed to be uniform along the length of the waterway. Usually, such simple flow conditions are only approached prior to an unsteady flow disturbance. Indeed, it is usually the unsteady flow disturbance (transient) that is of vital engineering significance. Among the most important causes of transient flows are the following:

- (1) Runoff from precipitation (rainfall event and/or snowmelt)
- (2) Transient flows released from reservoirs during operations for flood control, hydropower generation, recreation, and wildlife management, etc.
- (3) Tidal-generated waves
- (4) Dam-break floods
- (5) Wind-generated storm surges or seiches
- (6) Landslide-generated waves
- (7) Earthquake-generated tsunami waves
- (8) Irrigation flows affected by gates, pumps, diversions, etc.

The waterway may be naturally formed as in the case of streams, rivers, reservoirs, lakes, and estuaries, in which the cross-sectional geometry and bottom slope may vary from fairly uniform to very irregular. Waterways may be man-made such as canals, ditches, sewers, and flumes in which the cross-sectional geometry and bottom slope are usually uniform with perhaps small discontinuities.

The waterway may be a single channel or a network of connected channels. The network may be dendritic (tree-type) in which the branches (1) function as tributary channels, (2) function as distributary channels such as river deltas or irrigation canals (ditches). The network may consist of bifurcations such as the channels formed by islands; the bifurcations may be associated with bypass channels, sewer systems, or estuarial networks.

Unsteady flow models based on the complete Saint-Venant equations, or some simplified form thereof, provide a means for analyzing the flow of water along various waterways in numerous applications of engineering significance. Some of the applications are listed below:

- (1) Flood forecasting for real-time (a) warnings, (b) flood control operations, (c) evacuation, and (d) navigation information.

¹D. L. Fread, Senior Research Hydrologist, Hydrologic Research Laboratory, National Weather Service, Silver Spring, Maryland 20910

- (2) Flood prediction for developing (a) flood control systems (man-made reservoirs, bypasses, diversions channels, levees, spillways-uncontrolled, gated), (b) evacuation plans, (c) flood insurance assessments, (d) river improvements, (f) land use analyses, and (g) downstream assessment of reservoir releases (hydropower, flood control, dam-failure).
- (3) Design and real-time operation of sewer systems
- (4) Design and real-time operation of irrigation systems
- (5) Design of highway bridges and culverts
- (6) Water quality prediction (temperature, oil spill, BOD, etc.) in conjunction with other transport and reaction models
- (7) Prediction of alluvial river bed and roughness changes due to sediment transport in conjunction with sediment transport models
- (8) Streamflow-aquifer interactions in conjunction with groundwater models

Four applications are selected for presentation herein. They include: (1) a long, very mild sloping large river with a slow rising flood wave; (2) a dendritic river system consisting of four mild sloping large rivers with moderately rising flood waves and mutual backwater effects among the channels of the network; (3) a large, very mild sloping dendritic river system affected by a large tide at its mouth; and (4) a moderately sloping river subjected to a rapidly rising dam-break flood wave. These applications represent a wide spectrum of wave and channel characteristics for which the dynamic wave model is particularly well-suited and potentially the most accurate of the routing models.

Lower Mississippi. An unsteady flow model (DWOPER) was applied to a 291.7 mile reach of the Lower Mississippi River from Red River Landing to Venice shown schematically in Fig. 1 (Fread, 1978). Six intermediate gaging stations at Baton Rouge, Donaldsonville, Reserve, Carrollton, Chalmette, and Point a la Hache were used to evaluate the simulations. This reach of the Lower Mississippi is contained within levees for most of its length, although some overbank flow occurs along portions of the upper 70 miles. Throughout the reach, the alluvial river meanders between deep bends and relatively shallow crossings; the sinuosity coefficient is 1.6. The low flow depth varies from a minimum of 30 ft at some crossings to a maximum depth of almost 200 ft in some bends. The average channel width is approximately one-half mile. The average channel bottom slope is a very mild 0.000064. The Manning n varies from about 0.012 to 0.030. The discharge varies from low flows of about 100,000 cfs to flood discharges of over 1,200,000 cfs. A total of 25 cross sections located at unequal intervals ranging from 5-20 miles were used to describe the 291.7 mile reach.

The reach was first automatically calibrated for the 1969 spring flood. Time steps of 24 hours were used. Then, using the calibrated set of Manning n vs. discharge for each reach bounded by gaging stations, the 1969 flood was simulated using water elevation (stage) hydrographs for upstream and downstream boundaries at Red River Landing and Venice, respectively. The simulated stage hydrographs at the six intermediate gaging stations were compared with the observed hydrographs. The root-mean-square (RMS) error was used as a statistical measure of the accuracy of the calibration. The RMS error varied from 0.17 - 0.36 ft with an average value of 0.25 ft.

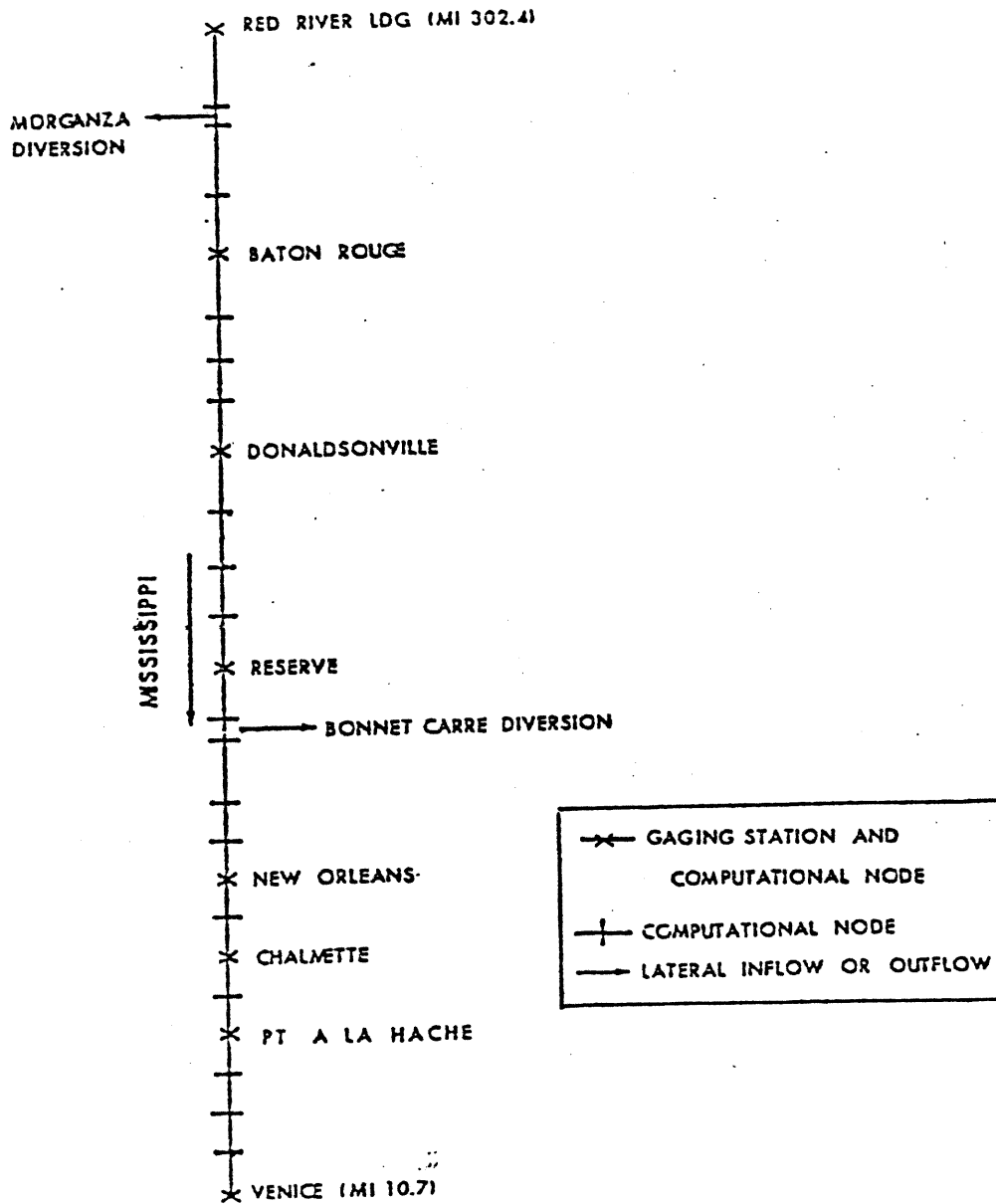


Figure 1. Schematic of Lower Mississippi River.

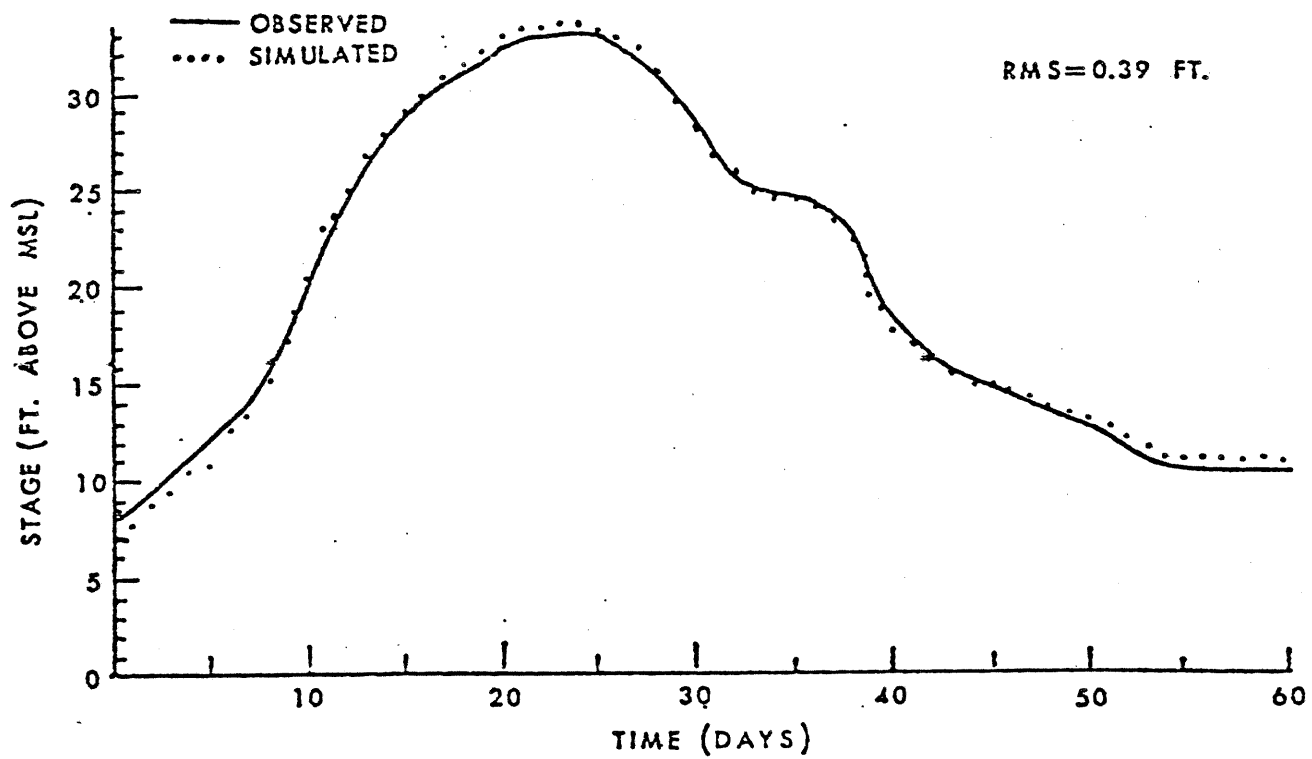


Figure 2. Observed vs. simulated stages at Baton Rouge for 1966 flood.

Several historical floods from the period 1959-1971 were then simulated using the calibrated Manning n values obtained from the 1969 flood. An example of simulated vs. observed stages is shown in Fig. 2 for the 1966 flood. Average RMS errors for all six stations for each of the simulated floods are shown in Table 1. The average RMS error for all the floods was 0.47 ft. This compares with 0.25 ft for the calibrated flood of 1969, indicating that for this reach of the Mississippi there is not a significant change in the channel roughness from one flood event to another. A calibration run required 7 sec on an IBM 360/195 computer system while a normal simulation run required 6 sec.

Mississippi-Ohio-Cumberland-Tennessee System. A dendritic channel system consisting of 393 miles of the Mississippi-Ohio-Cumberland-Tennessee (MOCT) River System was also simulated using DWOPER. A schematic of the river system is shown in Fig. 3. Eleven intermediate gaging stations located at Fords Ferry, Golconda, Paducah, Metropolis, Grand Chain, Cairo, New Madrid, Red Rock, Grand Tower, Cape Girardeau, and Price Landing were used to evaluate the simulation.

In applying DWOPER to this system, the main channel was considered to be the Ohio-Lower Mississippi segment with the Cumberland, Tennessee, and Upper Mississippi considered as first-order tributaries. The channel bottom slope is mild, varying from about 0.000047 to 0.000095. Each branch of the river system is influenced by backwater from downstream branches. Total discharge through the system varies from low flows of approximately 120,000 cfs to flood flows of 1,700,000 cfs. A total of 45 cross sections located at unequal intervals ranging from 0.5 to 20 miles were used to describe the MOCT river system.

The MOCT system was calibrated to determine the n-Q relationship for each of 15 reaches bounded by gaging stations. Time steps of 24 hours were used. About 25 seconds of IBM 360/195 CPU time were required by DWOPER to perform the calibration; a simulation run required only about 15 sec. The flood of 1970 was used in the automatic calibration process. The average RMS error for all 15 reaches was 0.60 ft. Typical comparisons of observed and simulated stages for the Cairo and Cape Girardeau gaging stations are shown in Figs. 4 and 5, respectively.

Using the calibrated n-Q relations, the 1969 flood was simulated. Stage hydrographs at Shawneetown and Chester and discharge hydrographs at Barkely Dam and Kentucky Dam were used as upstream boundary conditions, and a rating curve was used as the downstream boundary condition at Caruthersville. The average RMS error for the 11 intermediate gaging stations was 0.56 ft.

Columbia-Willamette System. DWOPER was applied to the 130-mile reach of the lower Columbia River below Bonneville Dam, including the 25-mile tributary reach of the lower Willamette River. A schematic of the river system is shown in Fig. 6.

This reach of the Columbia has a very flat slope (0.000011) and the flows are affected by the tide from the Pacific Ocean. The tidal effect extends as far upstream as the tailwater of Bonneville Dam during periods of low flow. Reversals in discharge during low flow are possible as far upstream as Vancouver. A total of 25 cross sections located at unequal distance intervals ranging from 0.6 -12 miles were used to describe the river system. One-hour time steps were used in the simulations which required about 11 sec on an IBM 360/195 computer system.

Table 1. Summary of flood simulations in Lower Mississippi River
(Red River Landing to Venice) for the years 1959-1971.

| <u>Year</u> | <u>Average RMS error (ft.)</u> | <u>Peak discharge (1,000 cfs)</u> |
|-------------|------------------------------------|---------------------------------------|
| 1959 | 0.62 | 750 |
| 1960 | .31 | 850 |
| 1961 | .47 | 1,220 |
| 1962 | .61 | 1,155 |
| 1963 | .38 | 950 |
| 1964 | .51 | 1,140 |
| 1965 | .44 | 1,040 |
| 1966 | .38 | 1,090 |
| 1967 | .38 | 700 |
| 1968 | .36 | 980 |
| 1969* | .25 | 1,065 |
| 1970 | .91 | 1,080 |
| 1971 | .41 | 940 |

*Calibrated

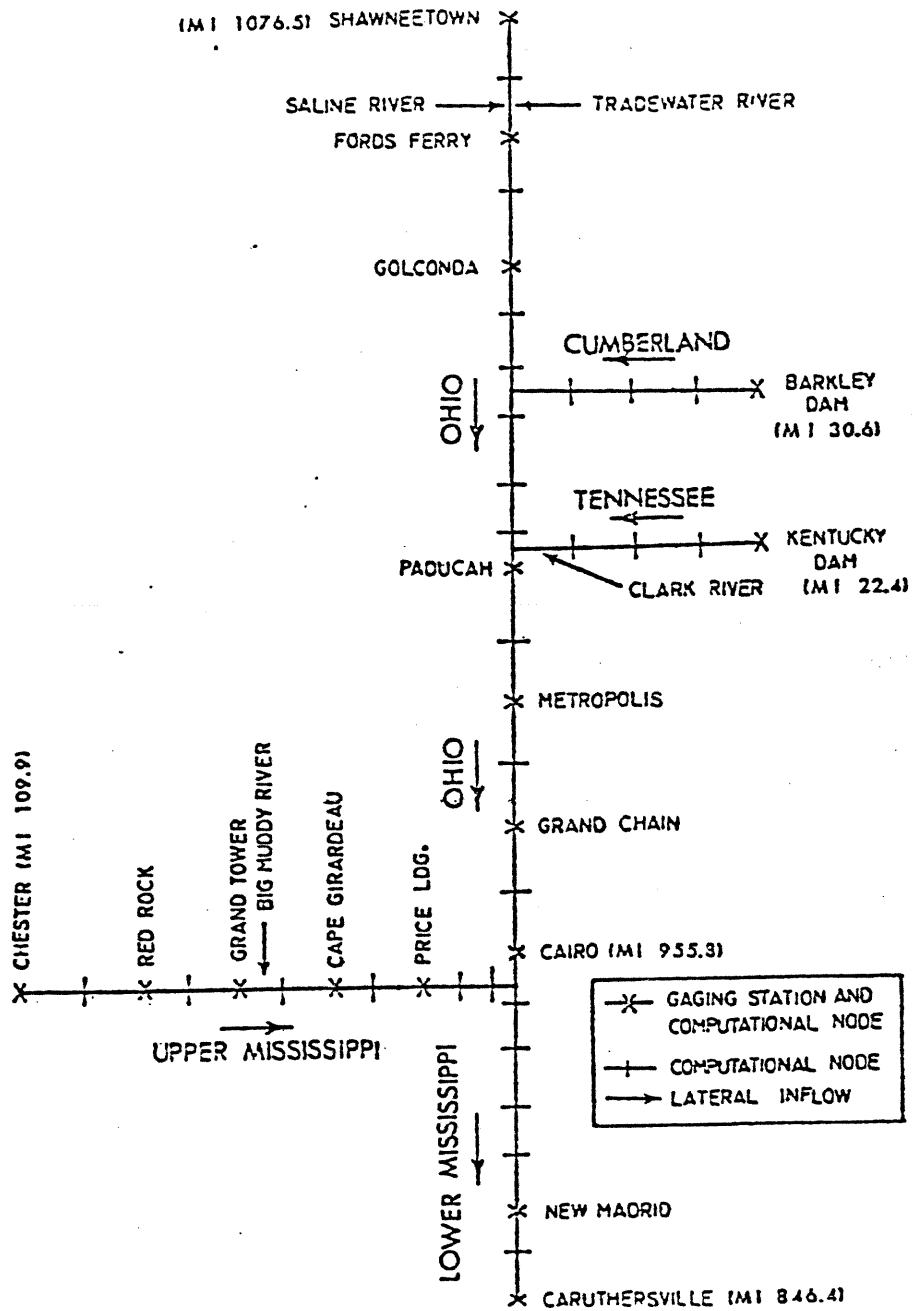


Figure 3. Schematic of Mississippi-Ohio-Cumberland-Tennessee (MOCT) River System.

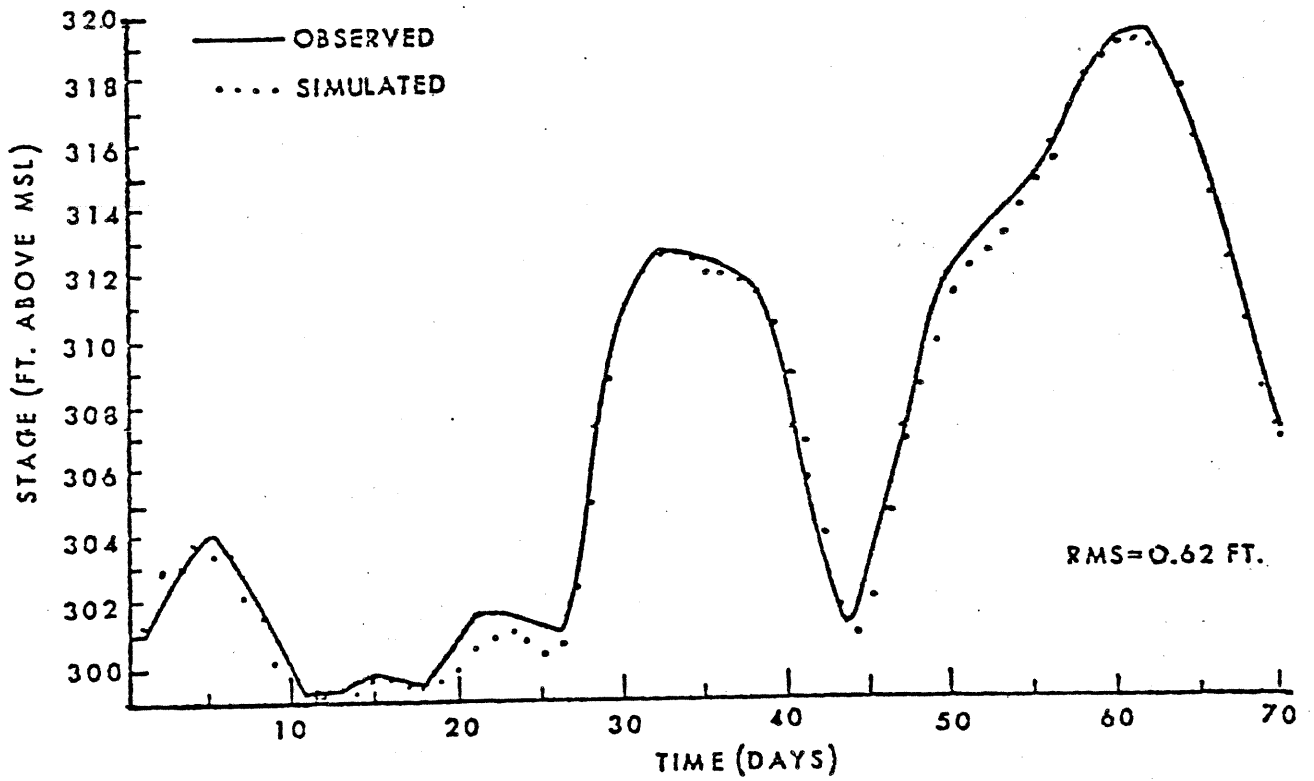


Figure 4. Observed vs. simulated stages at Cairo for 1970 flood.

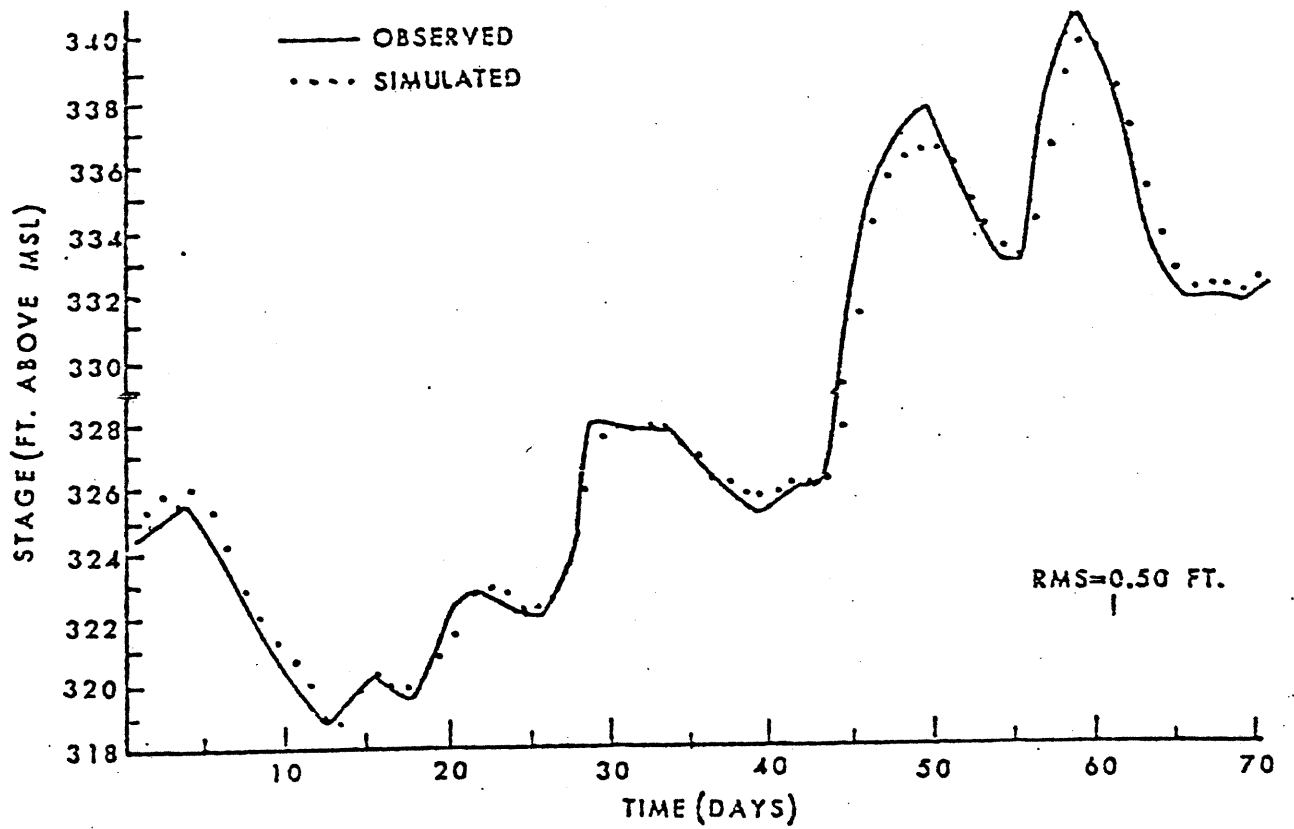


Figure 5. Observed vs. simulated stages at Cape Girardeau for 1970 flood.

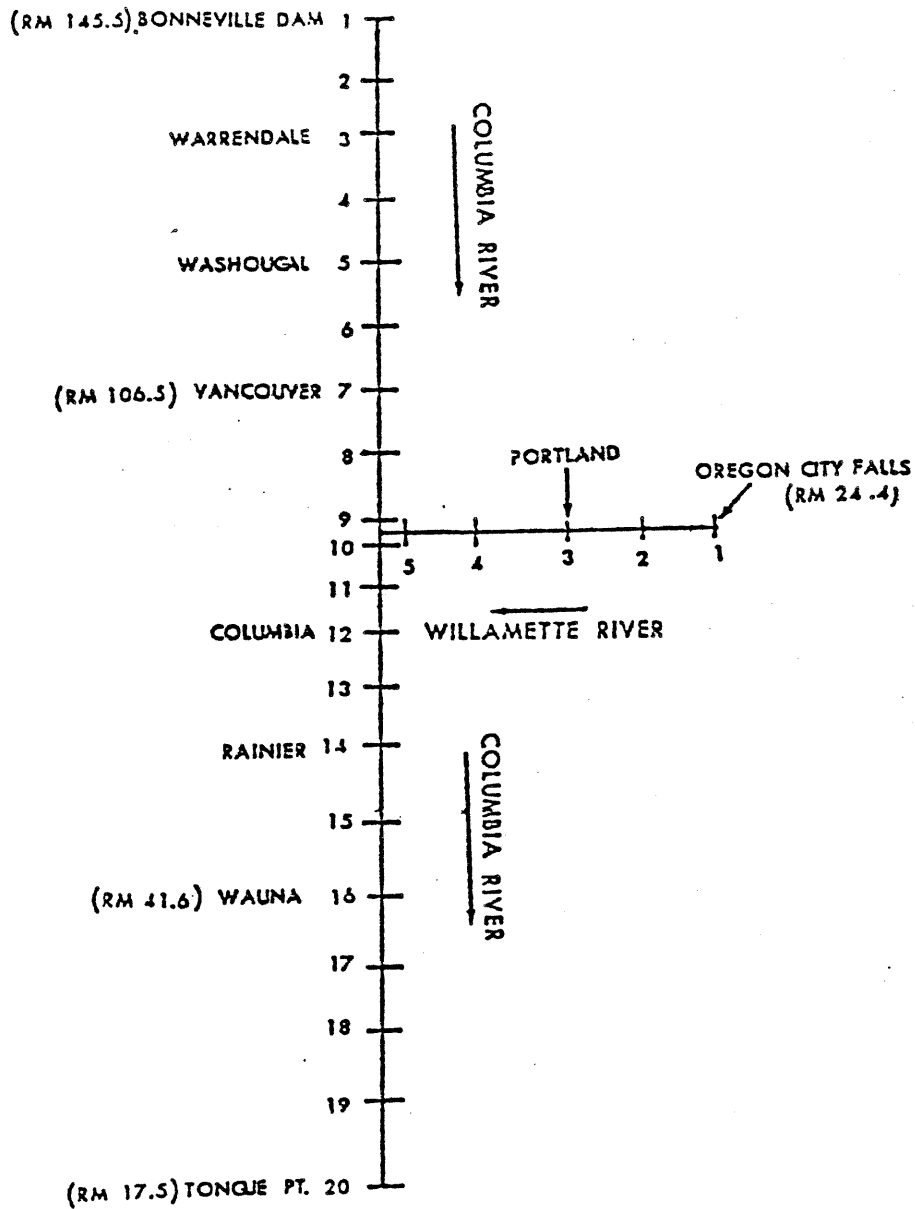


Figure 6. Schematic of lower Columbia-Willamette River System.

The system was first calibrated for a 4-day period in August 1973. Seven intermediate gaging stations at Warrendale, Washougal, Vancouver, Portland, Columbia City, Rainier, and Wauna were used along with the gaging stations at the extremities of the system, i.e., Bonneville, Oregon Falls, and Tongue Point. Another 5-day period in August 1973 was then simulated using the calibrated n-Q relations. Upstream and downstream boundaries were observed discharges and stages, respectively. The average RMS error for all stations in the simulation run was 0.21 ft. Some examples of simulated and observed stage hydrographs for Portland and Wauna are shown in Figs. 7 and 8, respectively.

Teton Dam-Break Flood. The Teton Dam, a 300-ft high earthen dam with a 3,000-ft long crest, failed on June 5, 1976, killing 11 people, making 25,000 people homeless, and inflicting about \$400 million in damages to the downstream Teton-Snake River Valley. Data from the U.S. Geological Survey provided observations on the approximate development of the breach, description of the reservoir storage, downstream cross sections and estimated values of the Manning's n approximately every 5 miles, indirect peak discharge measurement at three sites, flood peak travel times, and flood peak elevations. The inundated area is shown in Fig. 9.

The following breach parameters were used in DAMBRK (Fread, 1980) to reconstitute the downstream flooding due to the failure of Teton Dam:

$$\tau_{br} = 1.25 \text{ hrs}, \hat{b} = 150 \text{ ft}, z = 0, h_{bm} = 0.0, h_f = h_d = 261.5 \text{ ft}, Q = 16,000 \text{ cfs.}$$

The initial depth of the reservoir was 261.5 ft. Cross sections at 12 locations shown in Fig. 11 along the 60-mile reach of the Teton-Snake River Valley below the dam were used. The average bottom slope of the 60-mile reach is 0.00135. Five top widths were used to describe each cross-section. The downstream valley consists of a narrow canyon (approximately 1,000 ft wide) for the first 5 miles and thereafter a wide valley which was inundated to a width of about 9 miles. The estimated Manning n values vary from 0.028 to 0.047. Additional cross sections were interpolated such that computational reach lengths varied from 0.5 to 1.5 miles. The downstream boundary was assumed to be channel flow control as represented by a loop rating curve.

The computed outflow hydrograph is shown in Fig. 9. It has a peak value of 1,652,300 cfs, a time to peak of 1.25 hrs, and a total duration of about 6 hrs. The peak is about 20 times greater than the flood of record. The temporal variation of the computed outflow volume compared within 5 percent of observed values. The computed peak discharge values along the 60-mile downstream valley are shown in Fig. 10 along with three observed (indirect measurement) values at miles 8.5, 43.0, and 59.5. The average difference between the computed and observed values is 4.8 percent. Most apparent is the extreme attenuation of the peak discharge as the flood wave propagates through the valley. Losses due to infiltration and detention storage behind irrigation levees were assumed to vary from zero to a maximum of -0.30 cfs/ft and were accounted for by the lateral outflow (q).

The a priori selection of the breach parameters (τ_{br} and \hat{b}) causes the greatest uncertainty in simulating dam-break flood waves. However, sensitivity studies (Fread, 1980) show that large differences in the discharges near the Teton Dam rapidly diminish in the downstream direction. After 15 miles, the variation diminished to (+15 to -8 percent) for variations in \hat{b}

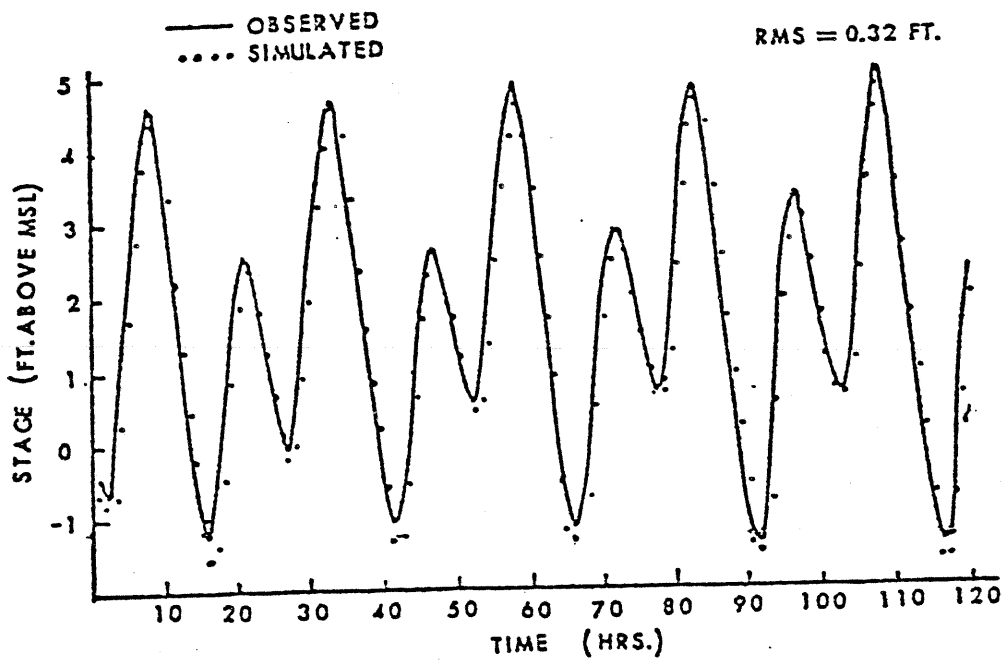


Figure 7. Observed vs. simulated stages at Wauna.

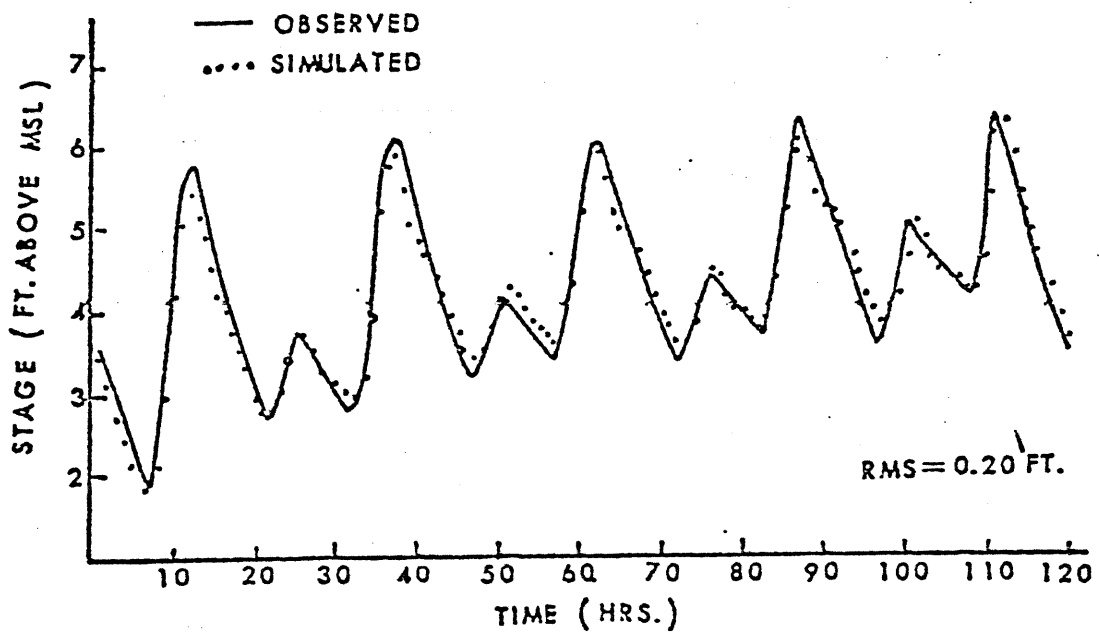


Figure 8. Observed vs. simulated stages at Portland.

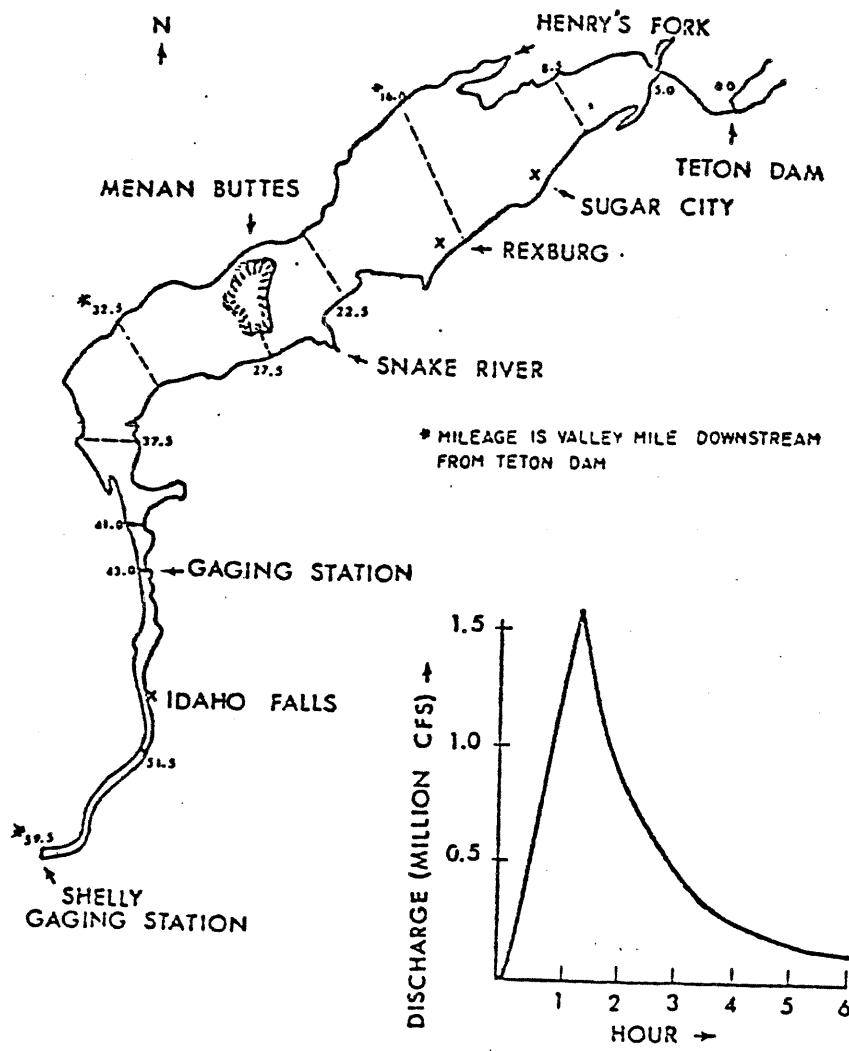


Figure 9. Outflow hydrograph and flood area downstream of Teton Dam.

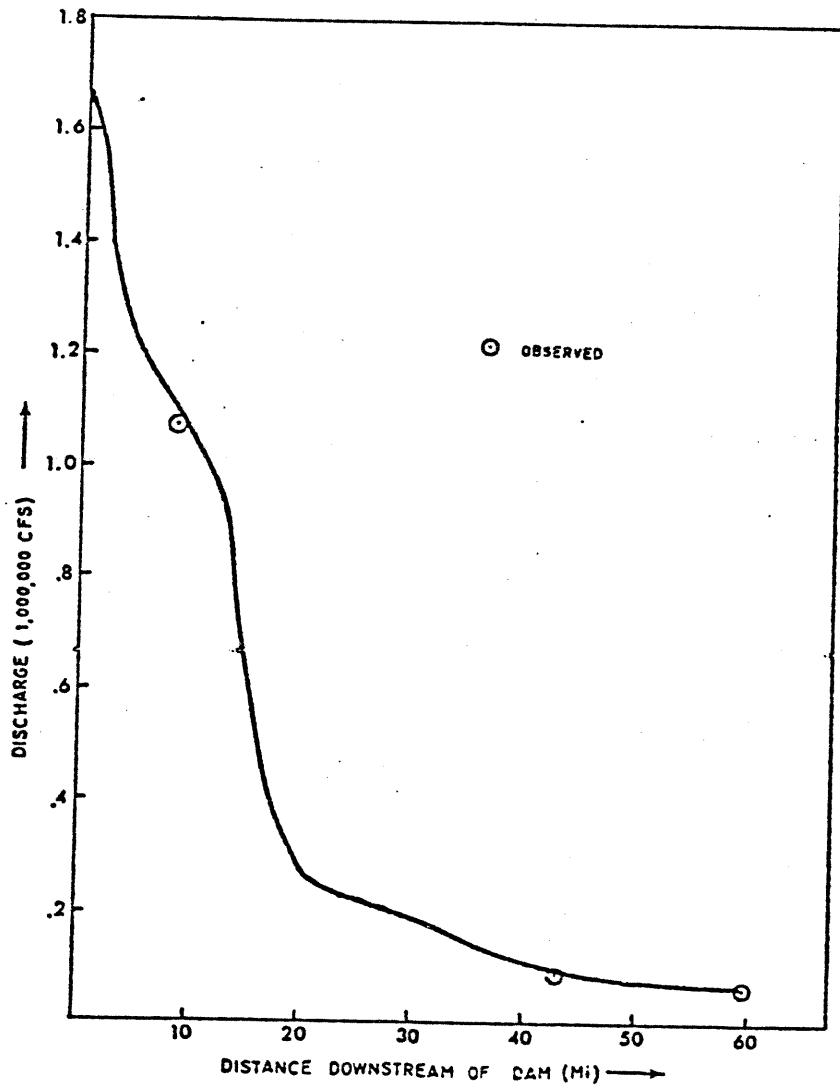


Figure 10. Profile of peak Discharge from Teton Dam failure.

of a factor of 2 and in τ_{br} of a factor from 0.3 to 2. The tendency for extreme peak attenuation and rapid damping of differences in the peak discharge is accentuated in the case of Teton Dam due to the presence of the very wide valley. Had the narrow canyon extended all along the 60-mile reach to the Shelly gage, the peak discharge would not have attenuated as much and the difference in peak discharges due to variations in \hat{b} and τ_{br} would be more persistent. In this instance, the peak discharge (cfs) would have attenuated to about 350,000 rather than 67,000 and the differences in peak discharges at mile 59.5 would have been about 27 percent, as opposed to less than 5 percent for the actual wide valley.

Computed peak elevations compared favorably with observed values. The average absolute error was 1.5 ft, while the average arithmetic error was only -0.2 ft. The computed travel time of the flood wave was compared with observed values at the locations of the discharge measurements; they differed by less than 10 percent.

A typical simulation of the Teton flood involved 78 Δx reaches, 55 hrs of prototype time, and an initial time step (Δt) of 0.06 hrs which was automatically increased gradually to 0.5 hrs as the wave propagated downstream and natural dispersion increased the time of rise. Such a simulation run required only 19 sec on an IBM 360/195 computer system.

REFERENCES

Fread, D.L. (1978). 'NWS operational dynamic wave model', in Verification of Mathematical and Physical Models, Proc. of 26th Annual Hydr. Div., Specialty Conf., ASCE, College Park, Maryland, pp. 455-464.

Fread, D.L. (1980). 'Capabilities of NWS model to forecast flash floods caused by dam failures', in Proc., 2nd Conf. on Flash Floods, Atlanta, Georgia, American Met. Soc., pp. 171-178.

